Time-Resolved Fluorescence of Flavin Adenine Dinucleotide in Wild-Type and Mutant NADH Peroxidase. Elucidation of Quenching Sites and Discovery of a New Fluorescence Depolarization Mechanism

Antonie J. W. G. Visser,*,† Petra A. W. van den Berg,† Nina V. Visser,† Arie van Hoek,† Harrold A. van den Burg,‡ Derek Parsonage,‡ and Al Claiborne‡

MicroSpectroscopy Centre, Department of Biomolecular Sciences, Wageningen Agricultural University, P.O. Box 8128, NL-6700 ET Wageningen, The Netherlands, and Department of Biochemistry, Wake Forest University Medical Center, Winston-Salem, North Carolina 27157

Received: May 6, 1998; In Final Form: September 1, 1998

Time-resolved polarized fluorescence experiments have been carried out on the FAD of tetrameric NADH peroxidase from *Enterococcus faecalis* and three mutant enzymes, C42A, C42S, and Y159A, respectively. In particular Tyr159 and, in part, Cys42 turned out to be the amino acids which are responsible for the strong dynamic quenching of flavin fluorescence, because two picosecond fluorescence lifetime components <150 ps are clearly present in the wild-type enzyme and in the Cys42 mutants, while only one picosecond lifetime <150 ps is present in the Tyr159 mutant. This observation is corroborated by the distance information obtainable from the known three-dimensional structure of the wild-type enzyme. Steady-state fluorescence spectroscopy indicated that the Tyr159 mutant has the same fluorescence yield as both Cys42 mutants suggesting that static fluorescence quenching prevails in the tyrosine mutant. Cys42 is the amino acid which is probably responsible for the static quenching in the wild-type enzyme and Y159A mutant. The time-resolved fluorescence anisotropy data showed a dependence on the emission wavelength. In case of proteins with Tyr159 present, less rapid depolarization is observed when the emission wavelength is at 526 nm, while depolarization of a few nanoseconds is more clearly visible at 568 nm. The rapid depolarization process was absent in the Y159A mutant irrespective of emission wavelength. The latter protein only showed a minor component of relatively long correlation time (>10 ns) which can be attributed to energy transfer among the flavins in the tetramer. The rapid ns depolarization is due to excited-state charge transfer between Tyr159 and flavin, which leads to a change of transition moment out of the plane of the isoalloxazine ring. The latter process contributes to a major extent to the observed fluorescence anisotropy decay and can be considered as an unusual source of fluorescence depolarization.

I. Introduction

Tetrameric NADH peroxidase (Npx) plays a key role in enterococcal oxygen metabolism,[1] catalyzing the two-electron reduction of hydrogen peroxide:

$$NADH + H^+ + H_2O_2 \rightarrow NAD^+ + 2H_2O$$

The enzyme contains, in addition to FAD, an unusual stabilized sulfenic acid derivative of Cys42 (Cys42−SOH), which catalytically cycles between reduced (Cys42−SH) and oxidized (Cys42−SOH) states in the reduction of H_2O_2.[2] The FAD plays an essential role in mediating the transfer of two electrons from NADH to the Cys42-SOH redox center, and the resulting Cys42-SH thiol (pK_a < 4.5) serves in a direct role as the nucleophile in the reaction with H_2O_2.[3,4] To characterize the spectroscopic and redox properties of NADH peroxidase the gene has been cloned, sequenced, and expressed in *Escherichia coli*.[5,6] Refined three-dimensional structures for the inactive Cys42−sulfonic acid derivative [E(Cys42-SO_3H)] have been published for both the free enzyme and its complex with NADH, at 2.16 and 2.4 Å resolutions, respectively.[7,8] Npx is structurally homologous to the well-characterized flavoprotein glutathione reductase (GR); the polypeptide chain folds into three domains involved in FAD-binding, NADH-binding, and in the tight GR-like "dimeric" interface between subunit pairs within the tetramer. With the three-dimensional structure has come the identification of a number of residues likely to play key catalytic and/or structural roles. The redox-active Cys42-SOH is joined in the active site by His10, which stabilizes both the Cys42-SOH redox center of the native enzyme and the transition state for the reaction of the Cys42-thiolate with H_2O_2.[9] Full analyses of the associated kinetic and redox properties have been published for both Cys42[3] and His10[9] mutants, and a preliminary report of the properties of an Arg303Met mutant has also appeared.[10] Arg303 is an important component of the domain zipper connecting FAD-binding and Central domains;[7] Arg303 also provides a hydrogen bond to His10-ND1 and is likely to stabilize the neutral form of the active-site His.[11] The structural and functional roles of these residues have been clarified even further with the recent 2.8 Å structure for the native E(Cys42-SOH) form of the peroxidase,[12] with the recent ^{13}C NMR analysis of

* To whom correspondence should be addressed at MicroSpectroscopy Centre, Department of Biomolecular Sciences, Laboratory of Biochemistry, Wageningen Agricultural University, Dreijenlaan 3, 6703 HA Wageningen, The Netherlands. Telephone: (31) 317-482862. Fax: (31) 317-484801. E-mail: Ton.Visser@laser.bc.wau.nl.

† Microspectroscopy Centre.

‡ Department of Biochemistry.

10.1021/jp982141h CCC: $15.00 © 1998 American Chemical Society
Published on Web 11/13/1998

the protein labeled with [3-^{13}C]Cys and [*ring*-2-^{13}C]His[13], and with the full kinetic analysis of the wild-type enzyme.[4]

The conformational dynamics of glutathione reductase from human erythrocytes have been characterized by time-resolved analysis of flavin fluorescence of the FAD prosthetic group.[14] Analysis of the time-resolved fluorescence intensity decay into a fluorescence lifetime distribution indicated a considerable conformational diversity. The majority of the enzyme (80−90%) is in a so-called "closed" conformation that appears to correspond to that observed in the crystal structure, in which Tyr197 functions as a lid to block access of reducing equivalents to the flavin; its fluorescence is quenched which is illustrated by a picosecond fluorescence lifetime component. It has been suggested that an excited-state complex with nearby Tyr197 is formed, which relaxes ultrarapidly mainly via a radiationless pathway to the ground state. Minor populations of GR molecules are characterized by longer fluorescence lifetimes (τ = 0.2−6 ns), probably due to a displacement of Tyr197 away from the isoalloxazine moiety, thus gradually alleviating the fluorescence quenching and leading to higher fluorescence efficiencies and longer lifetimes. It has also been proposed previously that these minor populations are important for catalysis, because in the "closed" form of GR, access of the NADPH substrate to the flavin is blocked by Tyr197. Therefore, structural fluctuations giving rise to more open conformations of GR may be important for interaction with NADPH. A pictorial view of the possible role of conformational dynamics in the catalysis of GR has been presented elsewhere.[15]

At this point it is worthwhile to put forward another fluorescence quenching mechanism. Instead of purporting a model of different protein conformers, Bajzer and Prendergast[16] proposed a model in which a single protein conformer contains different quenching sites. Such a model leads also to non-exponential fluorescence decay kinetics. If a "quenching" amino acid residue is removed and replaced by a "non-quenching" one, a less complex fluorescence decay is then certainly expected. Therefore, the use of site-specific mutants can corroborate or reject either this model or the distributed conformational model of Alcala et al.[17] The purpose of this study is to investigate whether the existence of conformational substates is a general property of flavoprotein disulfide-oxidoreductases. Alternatively, the model proposed by Bajzer and Prendergast[16] can be critically assessed. We have therefore performed time-resolved fluorescence intensity decay measurements of FAD in wild-type and site-selective mutants of Npx. The enzyme also has a tyrosine residue (Tyr159) located near the *re*-face of the FAD isoalloxazine; the structure of the E(Cys42-SO_3H)•NADH complex[8] shows that the aromatic side chain of Tyr159 swings out on NADH binding in much the same way as documented for Tyr197 on NADPH binding to human GR. The sulfur center of the redox-active Cys42-SOH in Npx is also a potential quencher of flavin fluorescence, and such quenching has been demonstrated in sulfur-containing flavin model compounds.[18] Four enzymes were selected for this study: the wild-type enzyme and three site-specific mutants in which Cys42 was changed to Ala (C42A) or Ser (C42S) and one in which Tyr159 has been replaced by Ala (Y159A). These mutant enzymes allow us to investigate whether Tyr159 is the most prominent quenching molecule for flavin fluorescence in Npx. Furthermore, comparisons of the fluorescence properties of these Npx proteins can confirm whether Cys42-SOH, next to Tyr159, can also act as a quencher of flavin fluorescence.

Bearing the concepts addressed above in mind, the time-resolved fluorescence properties of FAD bound in *E. coli* glutathione reductase have been recently investigated.[19] Site-selective GR mutants have been prepared in which the Tyr177 residue adjacent to the flavin has been replaced by either Gly or Phe. The flavin fluorescence decays are considerably slower than observed in the wild-type GR. Such observation is in agreement with the quenching-site model.[16] From analysis of the results it has been concluded that Tyr177 is a powerful dynamic quencher of flavin fluorescence. A dynamic quenching scheme has been proposed, in which the excited state of the flavin is rapidly deactivated by the abstraction of an electron from the adjacent tyrosine. In the flavin ground state the electron is then back-donated to the tyrosine and the original situation is restored. The idea has been put forward that such quenching mechanism would be a general mechanism in all flavoproteins having the flavin prosthetic group flanked by tyrosine or tryptophan residues. In this paper we will illustrate that Tyr159 in Npx has similar properties as Tyr177 in *E. coli* GR.

Energy transfer between the flavins in different subunits within dimeric flavoproteins such as lipoamide dehydrogenase or GR has been demonstrated by time-resolved fluorescence anisotropy analysis of the bound flavin cofactor.[14,15,20] The polarized fluorescence method has been able to furnish very detailed structural information yielding both interflavin distance and relative aromatic ring orientation. The final results were, within experimental error, identical to those obtained from the three-dimensional structures.[14,20] Another point of interest in the present study, therefore, concerns energy transfer among the FADs in the four subunits of Npx, as measured experimentally via time-resolved fluorescence anisotropy. These results can be compared with the information on the relative geometries of the flavins from the available wild-type and mutant crystal structures.[7,8,11,12] Because of the tetrameric quaternary structure, the anisotropy decay is expected to be more complex than in the dimeric structures of other disulfide-oxidoreductases such as lipoamide dehydrogenase.

Recent results of time-resolved fluorescence anisotropy with *E. coli* GR have revealed another interesting fluorescence depolarization mechanism.[19] The emission transition moment of the flavin moves out of the isoalloxazine plane, when a charge-transfer type of interaction between flavin in the excited state and tyrosine in the ground-state takes place. Such depolarization mechanism is distinctly different from the earlier proposed mechanism of rapid internal flavin flexibility in GR having a time constant of about 1 ns.[14] In the more recent publication[19] it is demonstrated that such a charge-transfer interaction provides a main contribution to the observed fluorescence anisotropy decay of FAD in GR. In this paper it is investigated whether the occurrence of such depolarization mechanism is a general property of this class of flavoproteins.

II. Materials and Methods

The preparation and characterization of the recombinant wild-type NADH peroxidase and the C42A and C42S mutants has been described.[3,6] The Y159A mutation was generated in the plasmid pNPR4, following the protocol described for the NADH peroxidase C42A and C42S mutants.[3] The 223 bp NciI/XbaI fragment from the mutant plasmid was ligated together with a 3.8 kb BbuI/XbaI fragment from pNPX12[6] and a 203 bp BbuI/NciI fragment from pNPX14[21] to give the pY159A expression plasmid. The final plasmid was checked by sequence and restriction analyses. The Y159A mutant protein was expressed in *Escherichia coli* JM109DE3 on induction with IPTG and was purified using the procedure developed for recombinant wild-

type NADH peroxidase.[6] Since the Y159A Npx was observed to lose activity on prolonged storage at −20 °C (attributed to oxidation of Cys42-SOH to Cys42-SO_2H and/or $-SO_3H$ forms), the pure protein was stored in aliquots at −80 °C.

For spectroscopic measurements all enzyme preparations had a concentration close to 10 μM with respect to FAD, on the basis of its extinction coefficient in NADH peroxidase and its mutants.[3,22] A value of $\epsilon_{446} = 11700\ M^{-1}\ cm^{-1}$ was determined for the Y159A mutant. Prior to experiments the proteins were chromatographed on a Biogel PGD-6 column (Bio-Rad Laboratories) equilibrated and eluted with the same buffer (50 mM potassium phosphate, pH 7.0, plus 0.6 mM EDTA).

Absorption spectra were obtained using a Hewlett-Packard 8452A diode array spectrophotometer, and steady-state fluorescence spectra were measured using an SLM Aminco-Bowman Series 2 spectrofluorimeter.[3] Fluorescence and fluorescence anisotropy decays were measured using the time-correlated single-photon-counting technique, which is summarized for applications in flavoprotein fluorescence in refs 14,15,19, and 20. The recent upgrading of the setup with another laser system as excitation source has been described in refs 19 and 23. The instrumental response function has a full width at half-maximum of ca. 50 ps, which makes registration of 5−10 ps lifetime components realistic. The laser excitation wavelength was set at 460 nm using a Coumarin 460 dye laser synchronously pumped by a mode-locked Nd:YLF laser. The excitation light was vertically polarized, while two components (parallel and perpendicular) of the fluorescence emission were collected alternately during the same time intervals. The (total) fluorescence decay was always composed of the sum of parallel and twice the perpendicular decays. The fluorescence was either detected at 567 nm using a combination of a line filter (half-bandwidth 12.6 nm) and a KV550 cutoff filter, or at 526 nm using a line filter (half-bandwidth 11.8 nm) and a KV520 cutoff filter (all filters were from Schott, Mainz, Germany). Using 526 nm detection, interference from Raman scattering of water was minimized. Using 460 nm excitation, Raman scattering is located at 551 nm; this was clearly visible when the mutant exhibiting the longest fluorescence decay (Y159A) was analyzed through a line filter transmitting at 557 nm. The results obtained at emission wavelength 526 nm were therefore selected for detailed fluorescence decay analysis as a function of temperature, since three out of four Npx enzymes exhibit ultrashort fluorescence decay components which would be difficult to distinguish from Raman scattering. It was also noticed that the longer lifetime components measured at longer emission wavelengths were exactly the same as the ones using 526 nm detection. The instrumental response function was obtained via an erythrosine B reference solution in water (fluorescence lifetime 80 ps as determined by Bastiaens et al.[14]). This so-called reference convolution method has been and still is effectively used by a number of researchers to eliminate wavelength dependency of the detection channel and to avoid any bias in response due to the different excitation and emission wavelengths and any differences in path lengths in excitation and emission modes of detection.[24] For fluorescence anisotropy decays the results obtained with both wavelengths (526 and 568 nm) were used, since no picosecond correlation times were seen. Fluorescence decays and fluorescence anisotropy decays were analyzed by the global analysis (GA) method with software obtained from Globals Unlimited (Urbana, IL). The global program has been described elsewhere.[25] Error estimation of the recovered lifetimes and correlation times has been performed by the exhaustive search method at the 67% confidence level as described in ref 25. Full details concerning the use of GA in flavoprotein research have been provided previously.[14,20,26] All analyses resulted in optimal fits with χ^2 (quality of fit parameter) close to unity and randomly distributed weighted residuals and autocorrelated residuals.

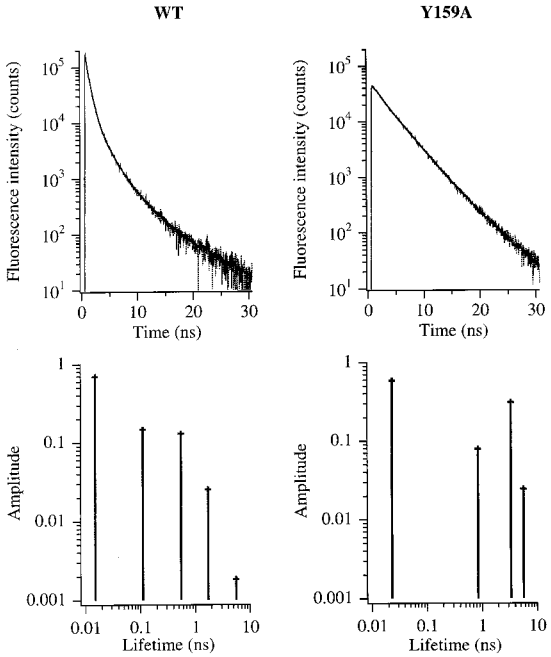

Figure 1. Experimental (···) and fitted (—) FAD fluorescence decays of wild-type Npx and the Npx mutant Y159A (top panels) and the global analysis in discrete lifetime components (lower panels) at 277 K.

III. Results and Discussion

Total Fluorescence Decay Analysis. In Figure 1 the time-resolved fluorescence profile is shown for FAD in wild-type and Y159A mutant NADH peroxidase in aqueous solution at 277 K. Especially in the fluorescence of the wild-type enzyme it can be clearly seen that the total emission decay has a strong heterogeneous character. Particularly in the initial part of the decay, a very rapid component can be distinguished (14 ps). The analysis using the GA method yields five discrete lifetimes between 5 ps and 6 ns for an optimal fit, which are presented as "sticks" of different amplitudes on the lifetime axis (Figure 1, lower panel, left). The shortest lifetime, which possesses the largest contribution, approaches the shortest time-resolution limit of the instrument. Since the steady-state fluorescence of FAD in NADH peroxidase is (almost) completely quenched, a possible explanation is that the ultrafast lifetime component is characteristic for the "closed" conformation of wild-type peroxidase (Tyr159 is at van der Waals distance from the FAD isoalloxazine; the closest approach is from phenolate oxygen of Tyr159 to the C4-carbonyl (C4F−O4F) of the isoalloxazine, *vide infra*). Analogous to glutathione reductase, the dynamic quenching of flavin fluorescence can be explained by the formation of a weak ground-state complex between the flavin and Tyr159. Such a complex can be light-excited, but will relax ultrarapidly and nonradiatively to the ground state thereby reducing the fluorescence lifetime to a few picoseconds. An excited-state reaction in which light-excited flavin abstracts an electron from the nearby tyrosine (Tyr177) has been proposed and substantiated in a recent paper dealing with *E. coli* glutathione reductase.[19] The presence of longer lifetime components provides evidence that not only in GR, but also in Npx,

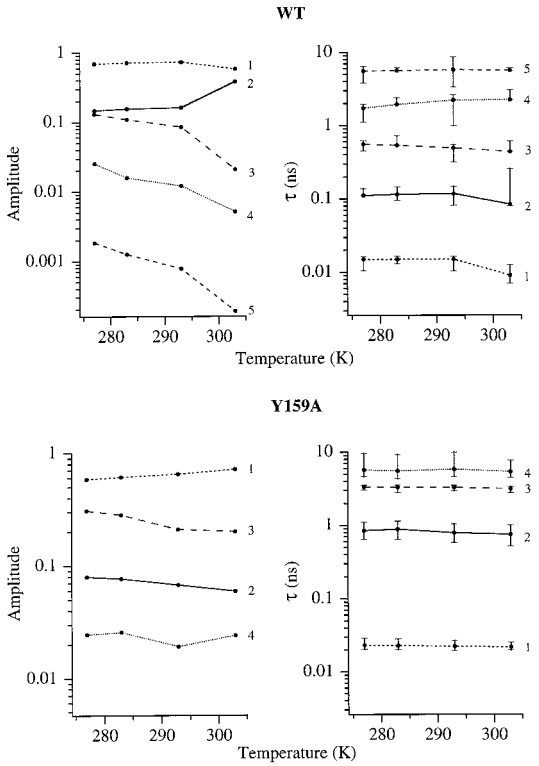

Figure 2. Temperature dependence for amplitudes and lifetimes (τ, ns) of the FAD fluorescence of wild-type Npx (top panel) and of the Npx mutant Y159A (lower panel). The lifetimes and corresponding amplitudes are numbered. The sum of the amplitudes is normalized to one. The confidence limits of the lifetimes have been determined by a rigorous error analysis as described in ref 25. For wild-type Npx a lower bound value was undefined in some cases (τ_3, τ_4 and τ_5 at 283 and 303 K; τ_2 at 277 K).

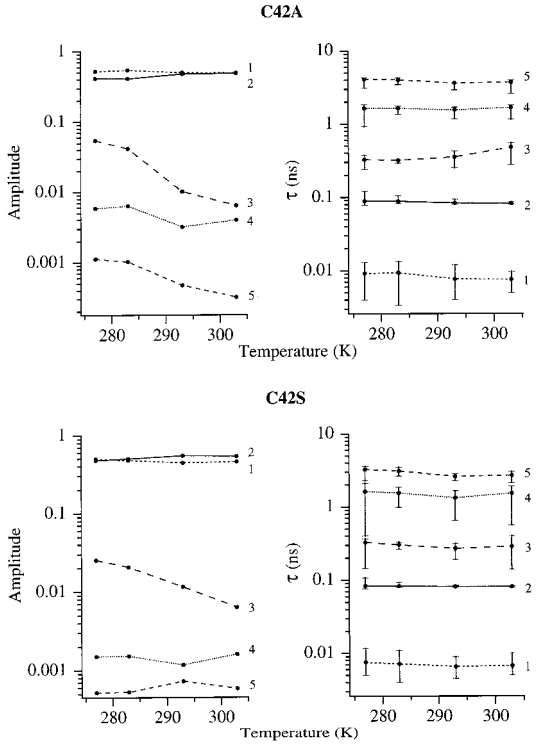

Figure 3. Temperature dependence for amplitudes and lifetimes (τ, ns) of the FAD fluorescence of Npx mutant C42A (top panel) and of Npx mutant C42S (lower panel). See legend to Figure 2 for details. All lifetimes have well-defined upper and lower bound values.

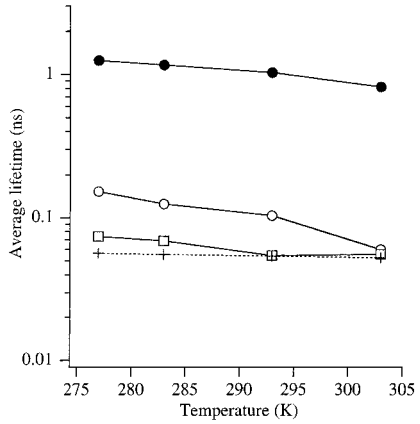

Figure 4. Temperature dependence for average fluorescence lifetimes ($\sum\alpha_i\tau_i$) for wild-type Npx (○) and three Npx mutants, C42A (○), C42S (+), and Y159A (●), respectively.

minor populations of peroxidase in more "open" structures exist. Mutation of Tyr159 into alanine clearly increased the short lifetime component to 23 ps indicating the presence of other quenching amino acids (see Figure 1). Again the "stick" spectrum, now consisting of four lifetimes, is presented in the same graph (Figure 1, lower panel, right). As will be discussed at the end of this paragraph, the most likely candidate for quenching is the sulfur atom of Cys42. The contribution of longer lifetimes is enhanced significantly, and the decay is less complex for the Y159A mutant. This experiment shows that Tyr159 is one of the most efficient dynamic quenchers of flavin fluorescence in Npx. The temperature dependence of decay parameters (between 277 and 303 K) are presented in Figures 2 (Npx and Y159A mutant) and 3 (C42A and C42S mutants). In contrast to the Y159A mutant, the C42A and C42S mutants exhibit two rapid lifetime components < 150 ps similar to those of wild-type enzyme (Figure 3). Both steady-state[3] and time-resolved fluorescence data of the four enzymes suggest a partial involvement of Cys42-SOH and a major involvement of Tyr159 in the quenching process. It is known from flavin model studies that the sulfur group can effectively quench flavin fluorescence.[18] Both wild-type and mutant enzymes also yield longer lifetimes (see Figures 2 and 3); it should be pointed out that these lifetimes account for nearly all of the total fluorescence, even though they represent only a small percentage in the total fluorescence decay.

The temperature dependence of the lifetime patterns of wild-type and mutant enzymes indicates that the lifetime components are more or less constant in the range 277−303 K (Figures 2 and 3). The smaller amplitudes exhibit some changes with temperature, but it should be realized that some amplitudes are significantly smaller than 0.1. The temperature dependence is also reflected in the first-order average fluorescence lifetimes $\sum\alpha_i\tau_i$ presented in Figure 4 (α_i are the amplitudes of the discrete lifetimes as given in Figures 2 and 3; $\sum\alpha_i = 1$). At temperatures higher than 303 K, the lifetime patterns of all proteins started to change gradually, and at 313 K a pronounced peak appeared at 2.0 ns (data not shown). This peak may well arise from some dissociated FAD, since such a lifetime component has been found previously in time-resolved fluorescence of FAD in aqueous solution.[27] This observation is confirmed by time-dependent fluorescence anisotropy experiments presented in the next section.

In principle, the first order average fluorescence lifetimes should scale with the fluorescence quantum efficiencies (collected in Table 1 for the data obtained at 293 K). Two apparent discrepancies are observed. The wild-type Npx and C42S and C42A mutants do not show large differences in average

TABLE 1: Fluorescence Quantum Efficiencies (q_{rel}) and Average Fluorescence Lifetimes ($\langle\tau\rangle$) of Npx and Three Mutants at 293 K

sample	q_{rel}[a] (%)	$\langle\tau\rangle$ (ns)
wild-type	2.2	0.104
Y159A	8.2	1.03
C42A	7.3	0.054
C42S	10.4	0.054

[a] Relative to the fluorescence quantum efficiency of free FAD.

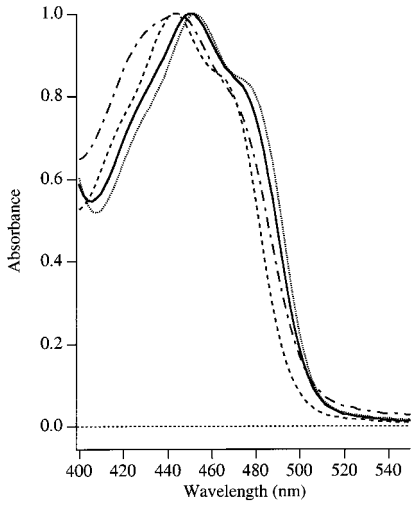

Figure 5. Absorption spectra of wild-type Npx (—) and three mutants, C42S (− −), C42A (•••), and Y159A (−•−), respectively, in the range 400−550 nm. Maxima are scaled to 1.0 for clarity. The temperature was 293 K.

fluorescence lifetime, but wild-type Npx has the smallest quantum efficiency. This observation suggests that there must be an additional quenching mechanism operating in the wild-type enzyme which is probably static quenching. The time-resolved fluorescence data indicate that Tyr159 is the main molecular source of dynamic flavin fluorescence quenching because the Y159A mutant has the longest average fluorescence lifetime. On the other hand, the fluorescence efficiency of all three mutant enzymes is similar (Table 1). As in the wild-type Npx, the Y159A mutant shows a considerable amount of static quenching. Cys42 is then probably the responsible amino acid for the static quenching. Such quenching has also been postulated to describe the flavin fluorescence quenching in thioredoxin reductase which is presumably due to the proximity of a serine residue which can form a hydrogen bond with the flavin.[28] Any differences in fluorescence intensities between the flavin in the four Npx proteins are connected to minor changes in the relative geometries (distances, orientations) of flavin and quenching molecules. Moreover, site-selective amino acid mutations in Npx, in the vicinity of the FAD cofactor, can also induce changes in the direct microenvironment of the flavin. This is clearly illustrated in the 400−550 nm absorption spectra of FAD in wild-type Npx and the three mutants, showing distinct differences in wavelength maxima and vibronic resolution (Figure 5). The wild-type Npx and the C42A mutant exhibit similar absorption spectra with a pronounced vibronic shoulder at 476 nm and an absorbance maximum at 452 nm. The other two Npx mutants, Y159A and C42S, do not show this pronounced shoulder, while the absorption maximum is shifted to 444 nm. At this stage it is not clear why the light absorption differences of C42A and C42S are so pronounced, while the time-resolved flavin fluorescence properties are similar.

When the two available crystal structures (the 2.16 Å structure of the inactive E(Cys42-SO_3H) peroxidase form of Stehle et al.[7] and the 2.8 Å structure of the native E(Cys42-SOH) peroxidase of Yeh et al.[12]) are examined, the following features become apparent. The phenolate oxygen of Tyr159 is closest to the same three atoms of the FAD isoalloxazine in each of the two structures: these are the O4 oxygen (3.3 and 3.5 Å, respectively), the C4 carbon (3.8 and 3.7 Å, respectively), and the N3 nitrogen (4.3 and 3.9 Å, respectively). The sulfur atom of Cys42 is closest to four atoms in each of the two structures: these are the C4a carbon (3.5 and 3.7 Å, respectively), the C10a carbon (3.6 Å in both structures), the N10 nitrogen (3.9 and 3.8 Å, respectively), and the N5 nitrogen (3.8 and 4.0 Å, respectively).

Since the N5 nitrogen is likely involved as an electron input site in the flavin ground state,[29] this atom was chosen as the center of a sphere. In both structures, a 5.0 Å sphere using the flavin N5 nitrogen as the center includes only the Cys42-SOH and Tyr159. Similarly a 10 Å sphere about N5 identifies residues Leu40−Gln45, Arg132, Tyr159−Ile160 and Glu163, Ala297−Thr300, Ser327−Leu329, and Phe424′−Pro426′ (from the complementary subunit). From these geometries it appears that only Tyr159 and Cys42-SOH are likely involved in quenching of flavin fluorescence.

Multiple quenching sites in conjunction with a heterogeneous flavin environment constitute a complex biomolecular system in which both the decay models of Alcala et al.[17] and of Bajzer and Prendergast[16] are equally plausible and can be operative at the same time, making distinctions very difficult. The Y159A mutant of Npx is strongly supporting the latter quenching model, because a quenching site is removed and the fluorescence decay becomes simpler (see Figure 1).

Fluorescence Anisotropy Decay Analysis. Experimental fluorescence anisotropy decays at 277 K, reconstructed from the individual polarized intensity decays, are presented in Figure 6 for the four proteins studied. Only the first 10 ns have been displayed because of the large noise in the tail of the curves. In all cases, however, the global analysis was carried out over the whole (parallel and perpendicular polarized) decay curves extending over 30 ns. Note that after about 15 ns not many photons are left in the total fluorescence decay of wild-type Npx (see Figure 1) and the two Cys mutants. The first conclusion that can be made is that the fluorescence anisotropy decay patterns of the Tyr159-containing Npx enzymes depend on the emission wavelength. The decay is slower at 526 nm than at 567 nm. At 567 nm a pronounced depolarization of the fluorescence takes place in wild-type Npx and the C42S mutant. The C42A mutant shows a slower depolarization at both emission wavelengths, but the same tendency is visible. The second conclusion is that the latter depolarization is not observed in the Y159A mutant. In contrast, the Y159A mutant exhibits a slow decay of small amplitude which is superimposed on the contribution of the apparently immobilized tetramer rotation (estimated to be 132 ns at 277 K from the Stokes−Einstein relation) on the 30 ns observation time window of the experiment.

Prior to a complete interpretation of the fluorescence anisotropy decay of FAD in Npx, another interesting phenomenological observation has been made. A peculiar time-dependent fluorescence anisotropy pattern of the Y159A mutant was observed at 313 K, when the temperature was raised from 277 to 313 K (Figure 7). The decaying part in this pattern can be explained by the presence of free FAD which rotates with a correlation time on the order of a few hundred picoseconds. This temperature-dependent experiment shows that this mutant loses its prosthetic group at elevated temperatures. Such a

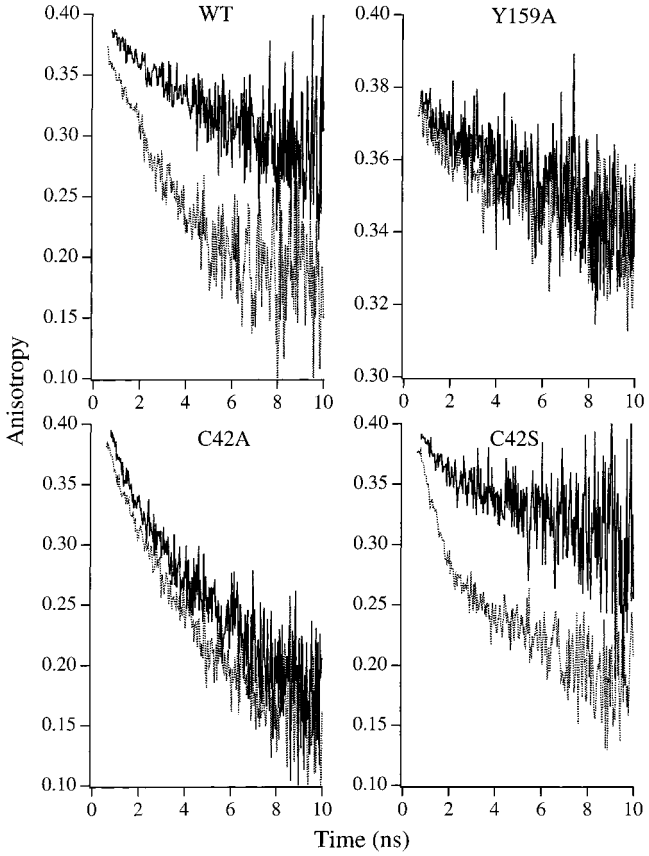

Figure 6. Experimental fluorescence anisotropy decays for wild-type Npx (WT) and three mutants, Y159A, C42S, and C42A, respectively, at 277 K and at two detection wavelengths. Dotted curves: 567 nm. Solid curves: 526 nm.

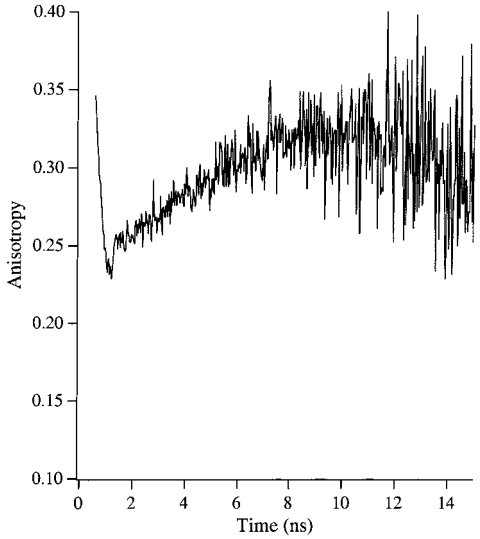

Figure 7. Experimental time-dependent fluorescence anisotropy of the Npx mutant Y159A at 313 K and at emission wavelength 567 nm. The rapid decay arises from dissociated FAD. The apparent rise in anisotropy is due to the contribution of Npx-bound FAD, which is immobilized on the observation time scale and which has fluorescence decay characteristics different from those of free FAD.

mixture of (time-dependent) anisotropies of free and Npx-bound FAD can only be analyzed with an associative fitting model.[15] Since this effect is most clearly present in the Y159A mutant and does not show up so evidently in the total fluorescence decay (*vide supra*), we have decided to present such a peculiar time-dependent fluorescence anisotropy pattern. Our conclusion is therefore that fluorescence anisotropy decay is a powerful

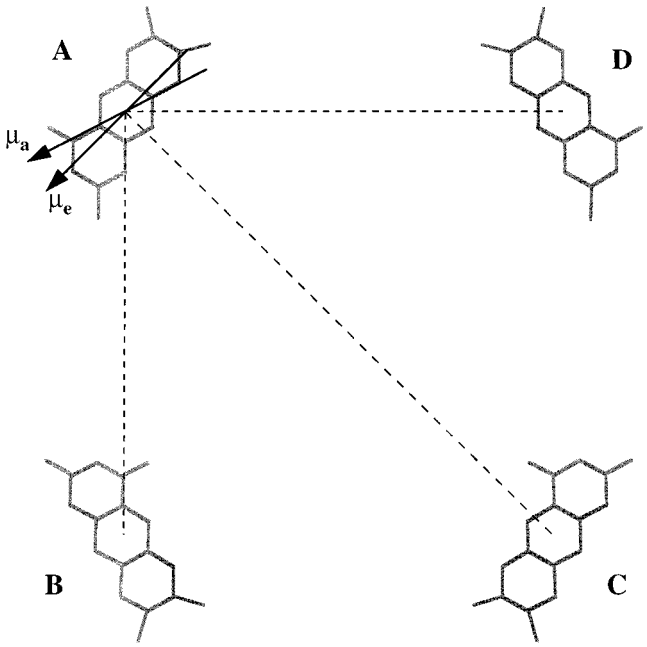

Figure 8. The geometry of the four flavin moieties in tetrameric Npx. The absorption (μ_a) and emission (μ_e) transition moments are also shown.

method to monitor the onset of FAD dissociation from flavoproteins. It is merely for this reason that the temperature-dependent measurements have been restricted between 277 and 303 K. Low values of fluorescence polarization of free flavin residues have already been determined by Weber in the early 1950s.[30]

Bastiaens et al.[14] have discussed the different sources of fluorescence depolarization: internal flexibility, overall rotation of the enzyme, and energy transfer between flavins in different subunits. It is important to note that, except for the Y159A mutant, in analogy to the situation in GR, the "carrier" signal for fluorescence anisotropy comes from the longer fluorescence lifetimes. We have strong evidence that three distinct depolarization processes are playing a role in the apparent fluorescence anisotropy decay of the three Tyr159-containing enzymes. The first process is a more rapid depolarization with a time constant of a few nanoseconds, observed at 567 nm. The other process is energy transfer among the four flavins in the tetramer, which is in the 10−20 ns range (*vide infra*). There is a third process which is overall rotation of the 200 kDa tetramer, but this process is very slow on the 30 ns time scale of the experiment and can be approximated using the Stokes−Einstein relation by a correlation time of 132 ns at 277 K and of 80 ns at 293 K. We will discuss the first two sources of flavin fluorescence depolarization starting with energy transfer.

The process of resonance energy transfer among the four flavins is very likely in a tetramer (Figure 8). Weber[31] very nicely showed that, when there are three distinct sites, two different rate constants for energy transfer (in such an apparently symmetric flavoprotein) must be considered: between adjacent flavins (A,B; A,D) and between flavins positioned at the diagonal (A,C) (see Figure 8). The expression for the contribution of energy transfer in the anisotropy decay then becomes[32]

$$r(t) = w_1\{A_1 \exp(-2k_T^{A}t) + A_2\} + w_2\{B_1 \exp(-2k_T^{C}t) + B_2\} \quad (1)$$

where k_T is the rate constant of energy transfer (for a dimer,

TABLE 2: Geometry of Flavin Rings and Rate Constant of Flavin-to-Flavin Energy Transfer of Wild-Type Npx and Spectral Overlap Integrals of Wild-Type Npx and Three Npx Mutants

donor−acceptor pair[a]	distance (R)	orientation factor (−)	transfer rate constant (k_T)
A,B	40.9 Å	3.6	40.7 MHz
A,C	60.2 Å	0.1	0.1 MHz
A,D	44.4 Å	0.8	5.5 MHz

Npx form	overlap integral (J)
wild-type	3.1×10^{-15} cm^3/mol
Y159A	2.7×10^{-15} cm^3/mol
C42A	2.8×10^{-15} cm^3/mol
C42S	2.4×10^{-15} cm^3/mol

[a] See Figure 8 for notation.

$2k_T = 1/\phi_T$; ϕ_T is the transfer correlation time), and the superscripts denote the two types of geometries in the tetramer. A_2 and B_2 are constant terms whose values depend on the relative geometry of the two flavins (cf. ref 14). The weighting factors (w_1 and w_2) take into account the probabilities of occurrence of energy transfer between specific flavin pairs: energy transfer between adjacent flavins is twice more probable than between diagonally positioned ones. The Förster rate constant of energy transfer is given by (cf. ref 33):

$$k_T = 8.71 \times 10^{23} R^{-6} \kappa^2 n^{-4} k_r J \qquad (2)$$

where R is the actual distance (in Å), κ^2 the orientation factor, n the refractive index, k_r the radiative fluorescence rate constant (in s^{-1}) of the flavin, and J the integrated spectral overlap of flavin absorbance and fluorescence spectra (in cm^3/mol). The refractive index is chosen as $n = 1.3$, and the radiative rate has been determined previously $k_r = 0.056$ ns^{-1}.[34] From the known three-dimensional structure of Npx, the orientation factors and distances between the flavin rings can be evaluated for all three combinations (Table 2). The location of the absorption transition moment was taken from ref 35 and that of the emission moment from ref 14 (they are presented in Figure 8). Interestingly, the flavin rings located at the diagonal over the largest distance of 60.2 Å are nearly perpendicular to each other. In addition, the distances between the flavin neighbors are not the same (Npx is therefore from the point of view of the flavins not a symmetric tetramer). The overlap integrals have been determined from the spectral data for all proteins studied and are collected as well in Table 2. The rate constants of energy transfer can then be calculated for all three pairs in wild-type Npx and are listed in Table 2. The transfer rate constant for the A,B pair is largest ($k_T = 40.7 \times 10^6$ s^{-1}). This would imply a transfer correlation time ϕ_T ($=1/2k_T$) = 12.3 ns. On the other hand, the orientation factor $\chi^2 = 3.6$, which is similar to a situation where the transition dipole moments are almost parallel implying only a tiny amount of depolarization. The transfer rate constant for the A,D pair is much smaller ($k_T = 5.5 \times 10^6$ s^{-1}) leading to $\phi_T = 90$ ns. The orientation factor of the latter energy transfer process would lead to a distinct depolarization of the fluorescence. However, the transfer correlation time is of the same order of magnitude as that connected with tetramer rotation and the two sources of depolarization can never be distinguished. In other words, the two main contributions to the fluorescence anisotropy decay in the Y159A mutant are energy transfer and rotational motion of the tetramer, respectively. Since the depolarizing effects are so small for the Y159A mutant in the observation time window of 30 ns (see Figure 6), it is decided to fix the correlation times to the abovementioned values and determine the preexponential factors from a global analysis of the parallel and perpendicular polarized decay curves. This leads to an excellent fit to the data (collected in Table 3). The obtained values connected with energy transfer and overall rotation are fixed in the analysis of the fluorescence anisotropy decays at 567 nm of the other three Npx proteins, in which we assume that energy transfer among the flavins is independent from temperature. As outlined by Bastiaens et al.[14] for the case of fluorescence anisotropy decay of FAD in lipoamide dehydrogenase, we can obtain two molecular angles from a linear combination of the preexponential factors β:

TABLE 3: Results of Analysis of Fluorescence Anisotropy Decay Detected at 567 nm of Npx and Three Mutants

sample	β_1(−)	ϕ_1[a] (ns)	β_2[b] (−)	ϕ_2[b] (ns)	β_3(−)	ϕ_3[c] (ns)	χ^2 [d]
277 K							
wild-type	0.19	2.9 (2.2−3.9)	0.01	12.3	0.17	132	1.07
Y159			0.01	12.3	0.36	132	1.11
C42A	0.26	4.1 (3.3−5.1)	0.01	12.3	0.12	132	1.05
C42S	0.17	1.6 (1.3−1.9)	0.01	12.3	0.20	132	1.09
293 K							
wild-type	0.16	1.2 (0.9−1.6)	0.01	12.3	0.20	80	1.04
Y159A			0.01	12.3	0.36	80	1.15
C42A	0.21	3.0 (2.4−3.8)	0.01	12.3	0.16	80	1.15
C42S	0.16	0.7 (0.6−0.8)	0.01	12.3	0.22	80	1.09

[a] The standard errors for this parameter (obtained after error analysis as described in ref 25) are determined only and are listed within parentheses. [b,c] Fixed to this value at both temperatures. [d] Fixed to this value, but different for the two temperatures. [e] Quality of fit parameter.

$$\beta_1 + \beta_2 = {}^3/_5 \cos^2 \delta - \frac{1}{5} \qquad (3)$$

$$\beta_2 + \beta_1 = {}^3/_5 \langle \cos^2 \theta \rangle - \frac{1}{5} \qquad (4)$$

where δ is the intramolecular angle between absorption and emission transition moments and θ is the intermolecular angle between absorption and emission transition moments. The brackets denote an average over two angles which are not necessarily the same (see ref 14 for full discussion). From the analysis of the Y159A anisotropy data we determined $\delta = 13°$ and $\theta = 165°$. For lipoamide dehydrogenase these angles were $\delta = 15°$ and $\theta = 134°$.[14] The main conclusion from the energy transfer data in the Y159A mutant is thus that intermolecular transition moments are more parallel in Npx than in dimeric lipoamide dehydrogenase. This is confirmed by the high value of the orientation factor (see Table 2).

Instead of invoking internal mobility of the flavin as proposed in ref 14 for human GR, we put forward another depolarization mechanism which can explain the data of the Tyr159-containing enzymes. The flavin excited state, with Tyr159 at van der Waals distance from the flavin, has considerable charge-transfer character. Electron transfer from Tyr159 to the excited flavin is then accompanied by a change in direction of the emission transition moment of the charge-transfer excited state out of the plane of the isoalloxazine. This possibility is a novel source of depolarization, for the first time documented for *E. coli* GR.[19] The mutant in which Tyr159 is replaced by an alanine residue strongly supports this interpretation, because no short correlation time is seen any more (Figure 6). The values of the nanosecond

relaxation times have been collected in Table 3. Two aspects need to be addressed. First, what is the significance of the relaxation process connected with the rapid fluorescence depolarization and the different relaxation times observed in the four proteins? The phenomenon observed can be considered as a kind of chemical relaxation process. The surrounding amino acids, including Tyr159, should adjust themselves in a fluctuating protein matrix to the change in direction of charge. The characteristic time needed for this is the reorientational relaxation time. For the C42A mutant this is a slower process than for the other two Tyr159-containing proteins. This can be a matter of slightly longer Tyr159-isoalloxazine distance and/or wrong orientation of the Tyr159 ring with respect to the isoalloxazine plane. This matter can be solved if crystal structures of the C42A and C42S mutants are available. The fact that this relaxation process is more rapid at higher temperatures is in agreement with the concept of structural fluctuations which occur more frequently and are of larger amplitude at higher temperature. The second point that needs to be explained is the clear emission-wavelength dependence of the observed fluorescence depolarization (at least in wild-type Npx and the C42S mutant): the depolarization is faster at the red side of the emission band. Such an effect must be connected with the properties of the charge-transfer excited state. When the flavin in Npx is excited in the first absorption band, the first-excited singlet state is created which is immediately followed by formation of the charge-transfer excited state. It is then logical to assume that the charge-transfer excited state is stabilized with respect to the first-excited singlet state and hence is more red shifted. A systematic study of the emission-wavelength dependence of the fluorescence anisotropy would lead to firmer conclusions.

IV. Concluding Remarks

The fluorescence decay experiments indicate that fluorescence lifetime heterogeneity is not restricted to glutathione reductase; it is also a property of NADH peroxidase and is probably a general feature of flavin-containing enzymes of similar structure, containing a tyrosine residue in the flavin vicinity. The model of different quenching sites in one conformation is difficult to distinguish from a model with different conformers each with its own fluorescence lifetime. However, the replacement of Tyr159 by Ala definitely results in a simpler fluorescence decay pattern and hence a quenching site is removed. The role of structural fluctuations (which lead to conformational diversity and possible interconversion between substates) in catalysis by these enzymes can be explored by investigation of other mutant enzymes containing alterations in the active site. Tyr159 has a distinct tendency to donate an electron to light-excited flavin. Such an effect can explain the peculiar fluorescence depolarization hitherto not disclosed. The flavin emission transition moment moves out of the isoalloxazine plane when a charge-transfer complex is created in the excited state. Such a depolarization must be an intrinsic property of a molecular complex between the flavin and a residue which is able to donate electrons to excited-state flavin. We have previously assigned the observed depolarization to flavin mobility. This is not correct, since the effect takes place in a relatively rigid flavin environment. On the other hand, there is certainly a temperature-dependent effect on the observed fluorescence relaxation. The protein has in this case the role of providing the correct environment to optimize the electron-transfer process. This is a kind of dipolar relaxation mechanism which has been proposed for other molecular cases as well.[36] The presence of a tyrosine close to the flavin has been found in other flavoproteins (discussed in ref 19). There must be a special role associated with a tyrosine close to the flavin. This role can be 2-fold. The enzyme will be definitely more photostable because the flavin will deactivate its excited state very efficiently. Alternatively, the tyrosine may have a role in stabilizing the enzyme because a more "compact" active-site conformation is favored.

Acknowledgment. This work was supported by The Netherlands Foundation for Chemical Research, with financial aid from The Netherlands Organization for Scientific Research (A.J.W.G.V.), by National Institutes of Health Grant GM-35394 (A.C.), and by National Science Foundation Grant INT-9400123 (A.C.).

References and Notes

(1) Claiborne, A.; Ross, R. P.; Parsonage, D. *Trends Biochem. Sci.* **1992**, *17*, 183−186.

(2) Claiborne, A.; Crane, E. J., III.; Parsonage, D.; Yeh, J. I.; Hol, W. G. J.; Vervoort, J. *Flavins and Flavoproteins 1996*; Stevenson, K. J., Massey, V., Williams, C. H., Jr., Eds.; University of Calgary Press: Calgary, Canada, 1997; pp 731−740.

(3) Parsonage, D.; Claiborne, A. *Biochemistry* **1995**, *34*, 435−441.

(4) Crane, E. J., III.; Parsonage, D.; Poole, L. B.; Claiborne, A. *Biochemistry* **1995**, *34*, 14114−14124.

(5) Ross, R. P.; Claiborne, A. *J. Mol. Biol.* **1991**, *221*, 857−871.

(6) Parsonage, D.; Miller, H.; Ross, R. P.; Claiborne, A. *J. Biol. Chem.* **1993**, *268*, 3161−3167.

(7) Stehle, T.; Ahmed, S. A.; Claiborne, A.; Schulz, G. E. *J. Mol. Biol.* **1991**, *221*, 1325−1344.

(8) Stehle, T.; Claiborne, A.; Schulz, G. E. *Eur. J. Biochem.* **1993**, *211*, 221−226.

(9) Crane, E. J., III.; Parsonage, D.; Claiborne, A. *Biochemistry* **1996**, *35*, 2380−2387.

(10) Crane, E. J., III.; Claiborne, A. *Flavins and Flavoproteins 1996*; Stevenson, K. J., Massey, V., Williams, C. H., Jr.; Eds.; University of Calgary Press: 1997; pp 773−776.

(11) Mande, S. S.; Parsonage, D.; Claiborne, A.; Hol, W. G. J. *Biochemistry* **1995**, *34*, 6985−6992.

(12) Yeh, J. I.; Claiborne, A.; Hol, W. G. J. *Biochemistry* **1996**, *35*, 9951−9957.

(13) Crane, E. J., III.; Vervoort, J.; Claiborne, A. *Biochemistry* **1997**, *36*, 8611−8618.

(14) Bastiaens, P. I. H.; van Hoek, A.; Wolkers, W. F.; Brochon, J. C.; Visser, A. J. W. G. *Biochemistry* **1992**, *31*, 7050−7060.

(15) Bastiaens, P. I. H.; van Hoek, A.; Brochon, J. C.; Visser, A. J. W. G. *Proc. SPIE* **1992**, *1640*, 138−147.

(16) Bajzer, Z.; Prendergast, F. G. *Biophys. J.* **1993**, *65*, 2313−2323.

(17) Alcala, J. R.; Gratton, E.; Prendergast, F. G. *Biophys. J.* **1987**, *51*, 925−936.

(18) Falk, M. C.; McCormick, D. B. *Biochemistry* **1976**, *15*, 646−653.

(19) van den Berg, P. A. W.; van Hoek, A.; Walentas, C. D.; Perham, R. N.; Visser, A. J. W. G. *Biophys. J.* **1998**, *74*, 2046−2058.

(20) Bastiaens, P. I. H.; van Hoek, A.; Benen, J. A. E.; Brochon, J. C.; Visser, A. J. W. G. *Biophys. J.* **1992**, *63*, 839−853.

(21) Miller, H.; Mande, S. S.; Parsonage, D.; Sarfaty, S. H.; Hol, W. G. J.; Claiborne, A. *Biochemistry* **1995**, *34*, 5180−5190.

(22) Poole, L. B.; Claiborne, A. *J. Biol. Chem.* **1986**, *261*, 14525−14533.

(23) van Hoek, A.; Visser, A. J. W. G. *Proc. SPIE* **1992**, *1640*, 325−329. Leenders, R.; Kooijman, M.; van Hoek, A.; Veeger, C.; Visser, A. J. W. G. *Eur. J. Biochem.* **1993**, *211*, 37−45.

(24) James, D. R.; Demmer, D. R. M.; Verrall, R. E.; Steer, R. P. *Rev. Sci. Instrum.* **1983**, *54*, 1121−1130. Zuker, M.; Szabo, A. G.; Bramall, L.; Krajcarski; D. T. *Rev. Sci. Instrum.* **1985**, *56*, 14−22. van Hoek, A.; Visser, A. J. W. G. *Anal. Instrum.* **1985**, *14*, 359−378. Vos, K.; van Hoek, A.; Visser, A. J. W. G. *Eur. J. Biochem.* **1987**, *165*, 55−63.

(25) Beechem, J. M.; Gratton, E.; Ameloot, M.; Knutson, J. R.; Brand, L. In *Topics in Fluorescence Spectroscopy*; Lakowicz, J. R., Ed.; Plenum: New York, 1991; Vol. 2, pp 241−305.

(26) Bastiaens, P. I. H.; Mayhew, S. G.; O′Nualláin, E. M.; van Hoek, A.; Visser, A. J. W. G. *J. Fluorescence* **1991**, *1*, 95−103; Visser, A. J. W. G.; van Hoek, A.; Visser, N. V.; Lee, Y.; Ghisla, S. *Photochem. Photobiol.* **1997**, *65*, 570−575.

(27) Visser, A. J. W. G. *Photochem. Photobiol.* **1984**, *40*, 703−706.

(28) Mulrooney, S. B.; Williams, C. H., Jr. *Prot. Sci.* **1997**, *6*, 2188−2195.

(29) Platenkamp, R. J.; Palmer, M. H.; Visser, A. J. W. G. *Eur. Biophys. J.* **1987**, *14*, 393−402.

(30) Weber, G. *Biochem. J*. **1950**, *47*, 114−121.
(31) Weber, G. *J. Phys. Chem*. **1989**, *93*, 6069−6073.
(32) Tanaka, F.; Mataga, N. *Photochem. Photobiol*. **1979**, *29*, 1091−1097.
(33) Dale, R. E.; Eisinger, J.; Blumberg, W. E. *Biophys. J*. **1979**, *26*, 161−194.
(34) Visser, A. J. W. G.; Müller, F. *Helv. Chim. Acta* **1979**, *62*, 593−608.
(35) Johansson, L. B.-Å.; Davidsson, Å.; Lindblom, G.; Razi Naqvi, K. *Biochemistry* **1979**, *18*, 4249−4253.
(36) Demchenko, A. P.; Sytnik, A. I. *Proc. Natl. Acad. Sci. U.S.A.* **1991**, *88*, 9311−9314.